Gate-tunable Josephson diode effect in Rashba spin-orbit coupled quantum dot junctions

Debika Debnath and Paramita Dutta

Theoretical Physics Division, Physical Research Laboratory, Navrangpura, Ahmedabad-380009, India

We theoretically explore the Josephson diode effect (JDE) in superconductor/quantum dot (QD)/superconductor junction in the presence of a magnetic field and Rashba spin-orbit interaction (RSOI). We calculate the Josephson current in our QD junction using the Keldysh nonequilibrium Green's function technique. We show that JDE is induced in our chiral QD junction with a large rectification coefficient (RC) in the presence of RSOI and external magnetic field simultaneously. Interestingly, the sign and magnitude of the RC are highly controllable by the magnetic field and RSOI. For realistic RSOI strength in the presence of magnetic field and chirality, the RC can be tuned to be as high as 70% by an external gate potential, indicating a giant JDE in our QD junction. Our proposed QD-based Josephson diode (JD) may serve as a potential superconducting device component.

I. INTRODUCTION

Unidirectional operation mechanisms have made diodes an inevitable part of modern electronic devices, such as current rectifiers, spintronics, quantum computers, switching devices, etc. Experimental advancements have led the path of diode formation from a semiconductor diode [1] to the very recent fabrication of a superconducting diode (SD) [2]. In a breakthrough experiment, Ando *et al.* observed a superconducting diode effect (SDE) in a noncentrosymmetric Rashba superlattice by sandwiching Nb/V/Ta layers [2]. In the follow-up experiment, Baumgartner *et al.* showed supercurrent rectification through the magnetochiral anisotropy in a two-dimensional electron gas (2DEG) [3]. The reason behind this evolution toward the SDE is inscribed in the directional preference of dissipationless supercurrent, while the conventional diodes are entirely based on dissipative current [4]. Afterward, the tunability of the unidirectional supercurrent via the phase difference between superconductor leads has drawn the attention of the community and brought JDs to the forefront of research during the past couple of years [5–19]. The possibility of wide applications has further sharpened the questions related to achieving higher rectification with possible external tunabilities.

To realize JDE, both inversion symmetry (IS) and time-reversal symmetry (TRS) breaking have been utilized in the literature, leading to the asymmetric current-phase relation (CPR): $I_c(\Phi) \neq -I_c(-\Phi)$ [15,20,21]. IS-breaking differentiates the current carried by electrons from the hole counterpart. On the other hand, breaking of the temporal symmetry ensures that the flow of up-spin electrons differs from that of down-spin electrons. To break the IS, the presence of chirality [22] or spin-orbit interaction (SOI) [2] is worth considering. For TRS breaking, one of the most convenient ways is applying an external Zeeman field, which offers additional freedom for controlling the nonreciprocal current. Otherwise, introducing intrinsic magnetism is also helpful for obtaining the JDE [23,24]. Thus, depending on the ways of TRS breaking, JDs

are classified into two categories: (i) extrinsic JDs where the TRS is broken by external magnetic field or flux [25,26], and (ii) intrinsic JDs with intrinsically broken TRS without any external source of TRS breaking as supported by recent works [8,27]. In some works, JDE was explained in terms of finite momentum Cooper pairs where both TRS and IS are broken [10,26,28]. These findings have opened the possibility of achieving efficient JDs in various ways.

Several works have been done to show JDE considering a Rashba superconductor [2,29], van der Waals heterostructure [30], a topological insulator [18,31], Dirac semimetal [25,32], 2DEG [33], a single magnetic atom [34], a carbon nanotube [35], InSb nanoflag [36], normal metal [37], band asymmetric metal [38], topological superconductors [39,40]. etc. In addition to higher-dimensional systems, zero-dimensional QD has also been used to show JDE [22,41,42]. The context of QDs is very relevant since QDs are thoroughly explored in Josephson junctions (JJs) [20,42–47] due to their potential applications in quantum information [48], spin qubits [49], single-electron transport [50], spintronic devices [51], and also medical science and nanotechnology [52].

Very recently, Cheng *et al.* showed JDE in chiral QD-based JJ in the presence of an external magnetic field [22], while Sun *et al.* have studied JDE in QD-based JJ with magnetic impurity [41]. In the chiral QD, chiral asymmetry can be introduced through distortion, thus making it suitable for nonreciprocity [32]. However, the study of JDE in QD-based junctions is very limited. An extensive study is necessary to exploit QDs meticulously for JDE or other SDEs. Note that in Ref. [22], Cheng *et al.* have not considered any RSOI [53]. In reality, the presence of RSOI is anticipated in such junctions [45,54,55]. It not only breaks the spin degeneracy [56,57], but also the splitting due to RSOI is tunable [58,59] via an external electric field, which makes it perfect for studying the current. Very recently, Mao *et al.* have explored RSOI in superconducting nanowire to generate a spin diode effect [60].

With this motivation, we show JDE in a QD-based JJ where a QD with RSOI is coupled to two superconductor leads in the
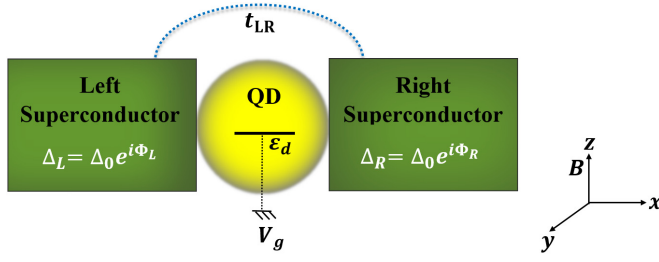
FIG. 1. The schematic diagram of QD-based JJ in the presence of an external magnetic field and gate voltage. A direct coupling between the superconducting leads is marked by the blue dotted line.

presence of an external magnetic field. To calculate the current flowing through the junction, we employ the nonequilibrium Keldysh Green's function method [61] where the self-energy and the Keldysh retarded and advanced Green's functions are found using Dyson's equation of motion [62]. We obtain the critical current for a range of superconducting phases, magnetic field, and RSOI. The energy of the single-level QD is controllable via an external gate-voltage [63]. We also study the effect of the gate voltages on the RC of our JD since gate-voltage can control the rectification phenomenon, as shown in a recent experiment [64]. Interestingly, the nonreciprocity of the critical currents, i.e., I_c^+ (positive critical current) $\neq I_c^-$ (negative critical current) in our chiral QD-based JD, is enhanced compared to the previously studied non-RSOI chiral QD junction [22]. Most interestingly, the sign and magnitude of the RC are tunable by the external magnetic field, RSOI, and the gate voltage.

We organize the rest of the article as follows. In Sec. II, we present our QD-based JD model and the Keldysh Green's function formalism. We present our results and discussions in Sec. III. Finally, in Sec. IV, we summarize our findings and conclude with some remarks.

II. MODEL AND FORMALISM

Our model for QD JJ is schematically shown in Fig. 1 where a QD is sandwiched between the left and right superconductor leads, denoted by L and R, respectively. An external magnetic field is applied along the direction perpendicular to the flow of the current (within the plane) as depicted in Fig. 1. For the sake of simplification, we consider the QD consisting of a single energy level that is tunable by an external gate-voltage V_g. A direct coupling between the two superconducting leads is also introduced to incorporate the effect of RSOI in the single level QD junction by virtually creating an extra path for electron transport. In the literature, this direct coupling between the leads has been extensively utilized theoretically and experimentally for decades to study the interference and tunneling [65–67].

We describe our QD-based JJ using the tight-binding Hamiltonian as

$$H = H_{QD} + H_{RSOI} + H_L + H_R + H_T + H_{LR}, \quad (1)$$

where H_{QD}, H_{RSOI}, $H_{L(R)}$, H_T, and H_{LR} represent the Hamiltonian for QD, RSOI, the superconducting left (right) lead, the
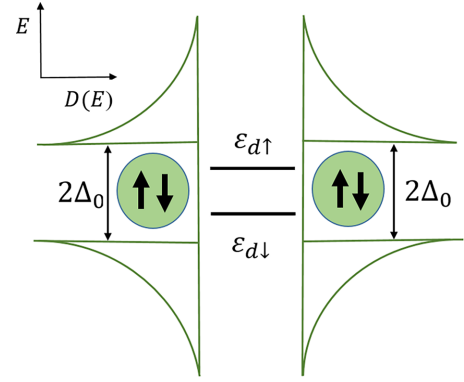
FIG. 2. Density of states $D(E)$ of the superconductor leads and the energy levels of the QD.

tunneling between the QD and leads, and the direct coupling between the two leads. These individual Hamiltonians read

$$H_{QD} = \sum_\sigma [(\varepsilon_d - eV_g + \sigma B + \sigma \lambda I) c_{d\sigma}^\dagger c_{d\sigma}, \quad (2)$$

$$H_{RSOI} = \alpha_R \sum_{d'd} \left[t_{d'd}^x (c_{d',\sigma}^\dagger c_{d,\sigma} - c_{d',\bar\sigma}^\dagger c_{d,\bar\sigma}) \right.$$
$$\left. + t_{d'd}^z (c_{d',\bar\sigma}^\dagger c_{d,\sigma} - c_{d,\bar\sigma}^\dagger c_{d',\sigma}) \right], \quad (3)$$

$$H_{L(R)} = \sum_{\alpha \in \{kL,k'R\},\sigma} \varepsilon_\alpha a_{\alpha\sigma}^\dagger a_{\alpha\sigma} + \sum_{\alpha \in \{kL,k'R\}} [\Delta_\alpha a_{\alpha\downarrow} a_{-\alpha\uparrow}$$
$$+ \Delta_\alpha^* a_{-\alpha\uparrow}^\dagger a_{\alpha\downarrow}^\dagger], \quad (4)$$

$$H_T = \sum_\sigma \left[\sum_{kL} v_L a_{kL\sigma}^\dagger c_{d\sigma} + \sum_{k'R} v_R a_{k'R\sigma}^\dagger c_{d\sigma} + \text{H.c.} \right], \quad (5)$$

$$H_{LR} = t_{LR} (a_{kL\sigma}^\dagger a_{k'R\sigma} + a_{k'R\sigma}^\dagger a_{kL\sigma}). \quad (6)$$

In Eq. (2), ε_d represents the energy level of the QD, which is tunable by the external voltage V_g (shown in Fig. 1), and B is the external magnetic field applied along the z-direction. Following Lenz's law, introducing the chirality in the QD generates an induced magnetic field which is proportional to the current flowing through the dot. The fourth term of Eq. (2) is responsible for the induced magnetic field, with λ being the proportionality constant [22]. The Pauli matrix σ acts on the spin degree of freedom. $c_{d\sigma}^\dagger$ ($c_{d\sigma}$) is the creation (annihilation) operator for the electrons in the QD where the notation d is used to identify the dot.

In Eq. (3), α_R is the strength of the RSOI. Due to the RSOI, the single energy level of the QD is split in two levels as shown in Fig. 2. Considering two states d and d' in the QD, the first term of Eq. (3) represents the hopping of same spin electrons between two different states and the second term corresponds to the spin-flip hopping. The second quantized form of the RSOI is derived [68] from the Hamiltonian given by

$$H_{RSOI} = \hat{y} \cdot \frac{\alpha_R}{\hbar} \left[\sigma \times \left(\mathbf{p} + \frac{e\mathbf{A}}{c} \right) \right], \quad (7)$$

where $\mathbf{A}$ is the magnetic vector potential and $\mathbf{p}$ is the momentum of electrons. Using the gauge $(0, Bx, 0)$, we can express

the hopping as $t_{d'd}^{x(z)} = \int dr \psi_{d'}^*(r) p_{x(z)} \psi_d(r)$, where $\psi_d(r)$ is the orbital wave function for the QD electrons.

In Eq. (4), ε_α with $\alpha \in \{kL, k'R\}$ denotes the on-site energy of electrons in both leads, while $a_{kL(k'R)\sigma}^\dagger (a_{kL(k'R)\sigma})$ is the creation (annihilation) operator of the electrons in the left (right) lead with momentum kL ($k'R$). The superconducting pair potential is denoted by $\Delta_{L(R)} = \Delta_0 e^{i\Phi_{L(R)}}$, where Φ_L (Φ_R) is the superconducting phase for the left (right) lead. The coupling strength between the left (right) superconductor and the QD is described by $v_L(v_R)$ in Eq. (5) and the direct tunneling coefficient between the two leads is represented by t_{LR} in Eq. (6) [44,68].

To simplify the total Hamiltonian, we now apply two unitary transformations. In one transformation, the superconducting phase $\Phi_{L(R)}$ and energy gap Δ_0 will be decoupled using the generator U_1, while in the other transformation based on the generator U_2, the effect of RSOI will be included in the tunneling current. Hence, the two consecutive unitary transformations are applied to Eq. (1) with the following generators:

$$U_1 = \exp\left[\sum_{kL(k'R)\sigma} \frac{i\Phi_{L(R)}}{2} a_{kL(k'R),\sigma}^\dagger a_{kL(k'R),\sigma}\right], \quad (8)$$

$$U_2 = \begin{cases} 1 & (x < x_L), \\ \frac{1}{\sqrt{2}} e^{-ik_R(x-x_L)\sigma} & (x_L < x < x_R), \\ \frac{1}{\sqrt{2}} e^{-ik_R(x_R-x_L)\sigma} & (x_R < x), \end{cases} \quad (9)$$

where $k_R = \alpha_R \frac{m^*}{\hbar^2}$. The transformed Hamiltonian reads

$$\tilde{H} = e^{U_2} e^{U_1} H e^{-U_1} e^{-U_2}. \quad (10)$$

The interlevel hopping and the spin-flip terms are neglected since our QD has a single energy level [44,68]. We obtain the transformed Hamiltonian as

$$\tilde{H} = \sum_{\alpha \in \{kL, k'R\}, \sigma} [\varepsilon_\alpha a_{\alpha\sigma}^\dagger a_{\alpha\sigma} + \Delta_0 a_{\alpha\downarrow} a_{-\alpha\uparrow} + \Delta_0^* a_{-\alpha\uparrow}^\dagger a_{\alpha\downarrow}^\dagger]$$

$$+ \left[\sum_{kL,\sigma} v_L e^{\frac{i\Phi_L}{2}} a_{kL\sigma}^\dagger c_{d\sigma} + \sum_{k'R,\sigma} v_R e^{\frac{i\Phi_R}{2}} a_{k'R\sigma}^\dagger c_{d\sigma} e^{-i\sigma\phi_{RS}}\right.$$

$$\left. + \text{H.c.}\right] + H_{QD} + H_{LR}. \quad (11)$$

Notably, the overall RSOI strength is now represented by the RSOI-induced phase factor ϕ_{RS} which appears in the tunneling part of the transformed Hamiltonian and it is related to the α_R by the expression $\phi_{RS} = \alpha_R \frac{m^*}{\hbar^2} l$, where l is the length scale of RSOI.

With this transformed Hamiltonian, the Josephson current in our QD-based junction can be found using the relation [69,70]

$$I = -e\left\langle \frac{dN_{L(R)}}{dt}\right\rangle = ie\langle [N_{L(R)}, \tilde{H}]\rangle, \quad (12)$$

where the number operator is given by $N_L = \sum_{kL,\sigma} a_{kL\sigma}^\dagger a_{kL\sigma}$. To calculate the current, we use the Keldysh nonequilibrium Green's-function formalism, which is one of the most efficient techniques to solve quantum transport problems. For

the Keldysh lesser Green's functions, we use the fluctuation-dissipation theorem [71,72] and obtain the Josephson current expression as

$$I = \frac{e}{\pi} \int d\epsilon \sum_\sigma \text{Re}\left[v_L e^{\frac{i\Phi_L}{2}} \{G_{dL,11}^<(\epsilon) + G_{dL,33}^<(\epsilon)\} \right.$$

$$\left. + t_{LR} \{G_{RL,11}^<(\epsilon) + G_{RL,33}^<(\epsilon)\}\right], \quad (13)$$

where $G_{ii}^<(\epsilon)$ is the iith element of the Fourier transformed time-dependent Keldysh Green's function $G^<(t)$.

For our model Hamiltonian in Eq. (1), the Keldysh lesser Green's function can be written as

$$G^< = \begin{pmatrix} G_{LL}^< & G_{LR}^< & G_{Ld}^< \\ G_{RL}^< & G_{RR}^< & G_{Rd}^< \\ G_{dL}^< & G_{dR}^< & G_{dd}^< \end{pmatrix}, \quad (14)$$

which is a 12×12 matrix in the spin $\bigotimes$ Nambu basis, and it follows that $G_{RL}^< = -(G_{LR}^<)^*$. Moreover, the Keldysh retarded Green's function can be expressed in terms of the self-energy using the Dyson equation of motion [62]: $G^r = g^r + g^r \Sigma^r G^r$, where g^r is the Keldysh retarded Green's function for the uncoupled QD and leads. The self-energy Σ^r carries all the information about the tunnelings. We refer to Appendix A for the details of the self-energy calculations. Finally, using Eq. (13), we calculate the Josephson current self-consistently considering the effect of the induced field.

To quantify the quality of the rectification by our JD, we define the diode RC as

$$\mathcal{R} = \frac{I_c^+ - |I_c^-|}{I_m} \times 100\%, \quad (15)$$

where we normalize the rectification by the mean current given by $I_m = (I_c^+ + |I_c^-|)/2$.

Throughout the rest of the manuscript, we consider the superconducting phases in the two leads as $\Phi_L = \Phi/2$ and $\Phi_R = -\Phi/2$ so that the phase difference becomes $\Phi_L - \Phi_R = \Phi$. We use the natural units where $m^* = 1$ and $\hbar = 1$, and we calculate the Josephson current I in units of $e\Delta_0$. Also, we set $v_L = v_R = 0.5\Delta_0$, $\lambda = 0.05$, $t_{LR} = 0.2\Delta_0$, and $eV_g = 0$ unless specified. We discuss the effects due to the change in the parameter values in the upcoming section. It is important to mention that we consider the magnetic field only along the perpendicular direction to maximize the rectification following the discussions in some recent works [22,29,73]. We show all the results only for symmetric leads where the pair potential is the same for both leads. A detailed discussion on the effects of asymmetric leads can be found in Appendix B.

III. RESULTS AND DISCUSSIONS

In this section, we present and discuss the behaviors of the current followed by the RC for the various parameters considered in our model.

A. Current-phase relation

We begin by referring to Fig. 3(a), where we show the CPR at a particular magnetic field for various Rashba phases. The phase difference between the two leads establishes a Josephson current with the CPR $I = I_c \sin \Phi$ similar to an ordinary JJ
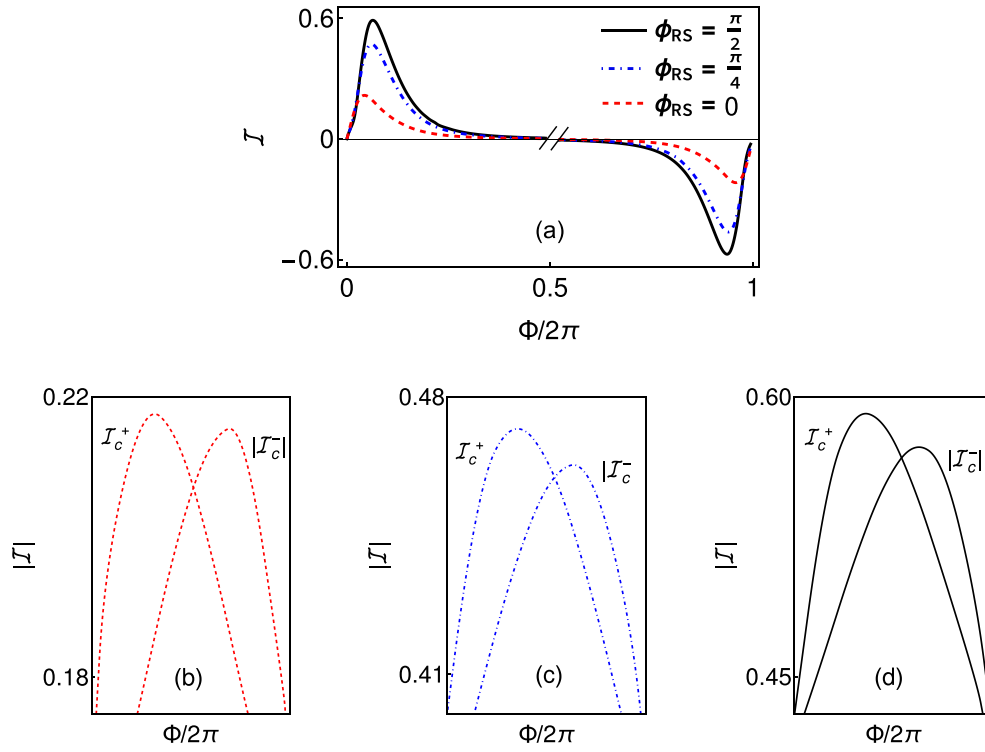
FIG. 3. (a) Josephson current (I) in units of $e\Delta_0$ as a function of superconducting phase difference (Φ) at $B = 0.6$ with and without Rashba phase. (b)–(d) A comparison between I_c^+ and $|I_c^-|$ for $\Phi/2\pi$ values along the x-axis given by (b) I_c^+: $0.02 \leqslant \Phi/2\pi \leqslant 0.07$ and $|I_c^-|$: $0.75 \leqslant \Phi/2\pi \leqslant 0.78$, (c) I_c^+: $0.03 \leqslant \Phi/2\pi \leqslant 0.07$ and $|I_c^-|$: $0.72 \leqslant \Phi/2\pi \leqslant 0.76$, and (d) I_c^+: $0.03 \leqslant \Phi/2\pi \leqslant 0.08$ and $|I_c^-|$: $0.71 \leqslant \Phi/2\pi \leqslant 0.75$, respectively.

as the Cooper pair tunnels through the channels of the QD (see Fig. 2). The Josephson current in our junction also follows $I(n\pi) = 0$, where $n = \pm 1, \pm 2, \ldots$ and so on. For a better understanding of the current profiles, we zoom around the peaks and skip showing the current around $\Phi/(2\pi) = 0.5$. To compare the magnitudes, we again show the positive (I_c^+) and the negative ($|I_c^-|$) critical currents separately in Figs. 3(b)–3(d) for Rashba phases $\phi_{RS} = 0$, $\pi/4$, and $\pi/2$, respectively. In Fig. 3(b), we observe that the positive critical current $I_c^+ = \max[I(0 < \Phi < \pi)]$ is not the same as the negative critical current $I_c^- = \max[-I(\pi < \Phi < 2\pi)]$, i.e., $I_c^+ \neq |I_c^-|$. This describes that for a particular phase difference, the forward current is different from the reverse current, indicating a JDE. At $\phi_{RS} = 0$, the JDE happens in the QD junction due to the presence of the external ($B \neq 0$) and induced field ($\lambda \neq 0$) that simultaneously breaks the TRS and chiral symmetry, respectively, similar to the results presented in Ref. [22]. However, the difference between I_c^+ and $|I_c^-|$, where $I_c^+ > |I_c^-|$, is very low in the absence of RSOI [see Fig. 3(b)].

Now, with finite RSOI ($\phi_{RS} \neq 0$), the magnitudes of the critical currents and also the asymmetry between them increase as depicted in Fig. 3. The inclusion of RSOI breaks the IS, which results in the enhancement of the nonreciprocity of the current, and thus the diode effect increases. Here, we want to point out that in the absence of any chirality ($\lambda = 0$) and magnetic field ($B = 0$), the CPR in a RSOI coupled QD junction follows the analytical form $I \simeq v_L \cos\frac{\phi_{RS}}{2}[\sin(\frac{\Phi+\phi_{RS}}{2}) + \sin(\frac{\Phi-\phi_{RS}}{2})]$ (see Appendix C for the derivation). We refer to

Appendix D for the results with $\lambda = 0$. Also, we show all the results for one particular coupling strength ($v_L = v_R$). Any change in the coupling strength will not affect the qualitative behavior of the current in our junction as long as it is less than the magnetic field.

To investigate the effect of the magnetic field and RSOI in more detail, we now plot the same for various magnetic fields in the absence and presence of RSOI in Fig. 4. We see that with the increase in the magnetic field, the critical currents and also the asymmetry between I_c^+ and $|I_c^-|$ increase. The behavior of the enhancement of the current with the
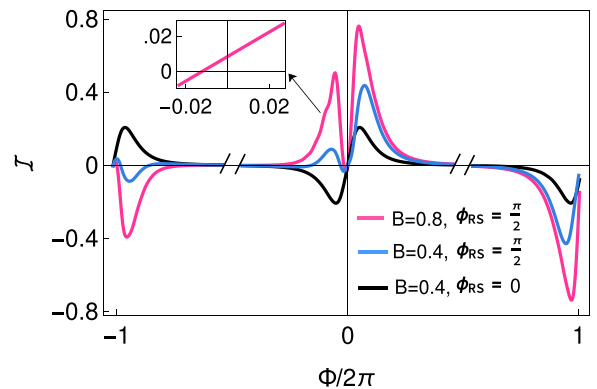
FIG. 4. Josephson current (I) in units of $e\Delta_0$ as a function of superconducting phase difference (Φ). Inset: Current profile around $\Phi = 0$.
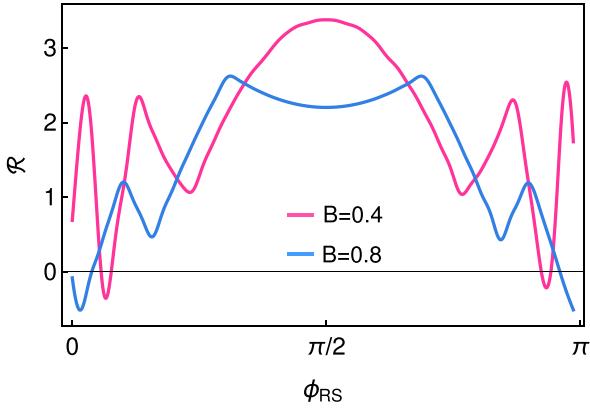
FIG. 5. Rectification coefficient ($\mathcal{R}\%$) vs Rashba phase (ϕ_{RS}).

increasing magnetic field is also found in the absence of RSOI [22]. In an ordinary JJ, the CPR follows $I(\Phi) = -I(-\Phi)$. Interestingly, in Fig. 4, we observe that this relation breaks down, i.e., $I(\Phi) \neq -I(-\Phi)$. We also find that in contrast to the usual 2π periodicity, i.e., $I_c(\Phi + 2\pi) = I_c(\Phi)$ found in an ordinary JJ, the symmetry around $\Phi = 0$ is lost in the presence of magnetic field and RSOI in the QD junction, resulting in 4π periodicity of the current. A small finite current is found to be present even at the zero superconducting phase difference, i.e., $I(\Phi = 0) \neq 0$ (see the inset of Fig. 4) where in an ordinary JJ, the CPR follows $I(\Phi = 0) = 0$. This indicates the appearance of an additional phase Φ_0 in the CPR and is referred to as the anomalous Josephson current in the literature [15,20,54,74,75]. The shifting of $I(\Phi = \Phi_0) = 0$ is also known as $\Phi_0 - JJ$. The combined effect of the IS and the TRS breaking is responsible for this anomalous supercurrent or equivalently the phase shift in our junction. We check that the shifting of the Φ_0 phase intensifies with the external magnetic field following $B/v_{L(R)} > 1$ [76]. This anomalous behavior of the current is explained in the literature in terms of the spontaneous breaking of TRS at $\Phi = 0$ [20,54,77–79].

B. Rectification without any gate voltage

Up to now, we have seen that the phenomenon of nonreciprocity follows $I_c^+ > I_c^-$. It indicates that the forward current

is preferred over the reverse one for all the parameter values considered so far. To analyze the rectification quality, we present the behavior of the RC using Eq. (15) for our QD-based JD as a function of ϕ_{RS} in Fig. 5. On the whole, RC of our JD initially increases and then decreases with the increase in Rashba phase. However, the detailed behavior of the RC depends on the magnitude of B. There appears an interplay between the RSOI strength and magnetic field for determining the value of RC. For illustration, at $B = 0.8$, the current in our QD-based JD increases as ϕ_{RS} increases from 0 to $\pi/2$. As ϕ_{RS} increases further, the RC reduces following a partial mirror symmetry with respect to $\phi_{RS} = \pi/2$. For a lower magnetic field strength like $B = 0.4$, we observe a saddle near $\phi_{RS} = \pi/2$. So, it is evident that the correlation between the B and ϕ_{RS} plays a vital role in determining the diode effect qualitatively and also quantitatively. Additionally, two more important observations are in order. The RC is low in this parameter regime. Interestingly, there exists a certain regime of RSOI, where we find negative values of the RC, which indicates that the backward current is preferred more than the forward one.

To understand the competitive effect of the RSOI and magnetic field on the diode quality, we now study the RC for broad parameter regimes of the magnetic field [$0 \leqslant B \leqslant 1$ in panel (a) and $-1 \leqslant B \leqslant 0$ in panel (b)] in the presence of RSOI by presenting a density plot of the RC in Fig. 6. Our observations are manifold. (i) The RC is finite but very low for $B = 0$. This is expected since external TRS breaking is not necessary for the chiral QD JDE [8,27,30,35] but the effective magnetic field cannot induce sufficiently large JDE in our RSOI coupled junction. (ii) RC varies with the strength of the magnetic field. (iii) The diode effect is sensitive to the direction of the applied magnetic field, i.e., $\mathcal{R}(B) \neq -\mathcal{R}(-B)$ when the directions of Rashba field and the supercurrent are unchanged. This is similar to the experimental results reported in Refs. [29,73]. The competitive effect of the magnetic field and the RSOI on the RC is more substantial when the magnetic field is applied along the $-z$-direction. (iv) Most interestingly, tuning the magnetic field and RSOI simultaneously, we can also tune the RC from positive to negative and vice versa. Comparing the two panels of Fig. 6, we observe that when the magnetic
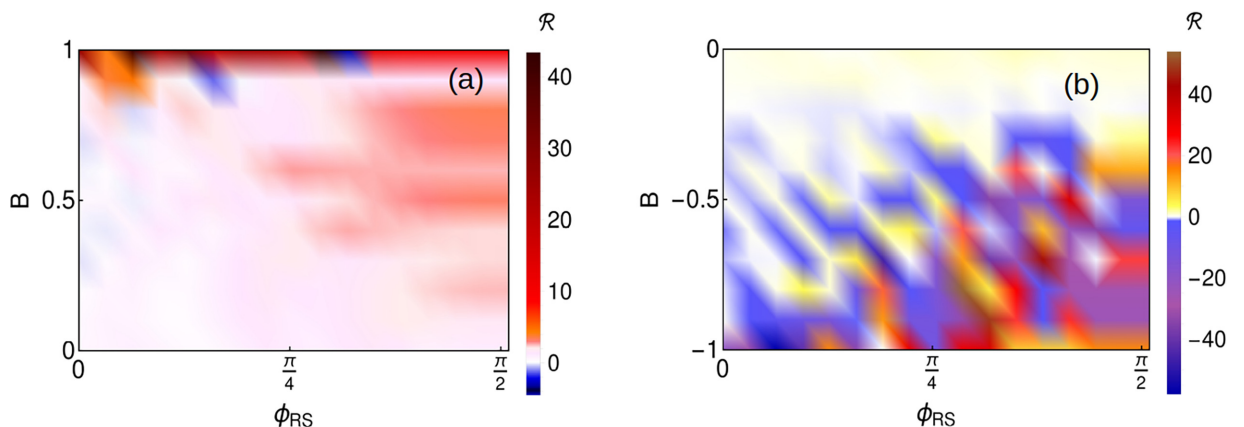
FIG. 6. Density plot of the rectification coefficient ($\mathcal{R}\%$) as a function of the Rashba phase (ϕ_{RS}) and magnetic field (B) applied along (a) the $+z$ direction and (b) the $-z$-direction.
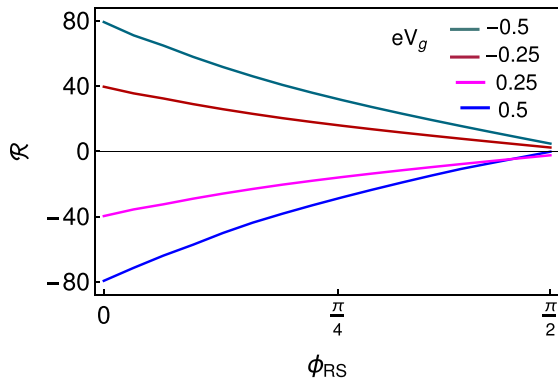
FIG. 7. Rectification coefficient ($\mathcal{R}\%$) vs Rashba phase (ϕ_{RS}) at $B = 0.4$.

field is applied along the $+z$-direction, higher values of the RC are achieved for strong magnetic fields only, whereas the RC is amplified for a relatively much weaker magnetic field for the same RSOI when it is applied along the opposite direction. (v) Overall, we find that maximum $\mathcal{R} \sim 42\%$ for $+B$ and $\sim 57.5\%$ for $-B$ can be achieved in our QD-based JD. We have checked that in the absence of any chirality ($\lambda = 0$), the diode RC can be as high as 43% due to only RSOI.

We explain the observations as follows. Introduction of the RSOI splits the QD energy level. When we simultaneously switch on the external magnetic field, it extends the energy level splitting considering the spins of the electrons. Therefore, the combined effect of the magnetic field and the Rashba generates several possibilities for the tunneling of the Cooper pairs from the left to the right superconducting lead. Hence, the correlation among both interactions results in ample possibilities or variations in the RC of our JD. It turns out that the direction of the supercurrent is strongly favored if the three vectors i.e., supercurrent, magnetic field, and RSOI, lie along the Cartesian coordinates (clockwise), which happens in the $+B$ direction in our setup. For $-B$, there are more fluctuations in the current with the sign of RC being sensitive to the strength of the magnetic field for any RSOI. It is essential to mention that the qualitative nature of the RC with the change in the direction of the external magnetic field from $-z$ to $+z$ matches well with the experimental study on SDE on epitaxial Al-InAs JJ, where the JDE due to strong RSOI is studied in the presence of an external magnetic field [73].

Before we proceed further, we comment on the direct coupling. In our JJ model, we consider a single energy level in the QD. For the single energy level, an external direct coupling between the two leads via t_{LR} is necessary to include the Rashba effect in our system [20,44]. This coupling opens up a pseudochannel for the electron to tunnel. In reality, since a single QD is a very small region, it is highly likely to have a direct coupling between the two leads. Eventually, the strength of this direct hopping has a significant effect on the RC, which we discuss in Appendix E.

C. Gate tunability of the diode effect

Up to now, all results have been shown only for the gate voltage $eV_g = 0$. In Fig. 7, we show the RC as a function

of the Rashba phase for various gate voltages. The applied gate voltage tunes the QD energy levels. We find that by only tuning the gate voltage, it is possible to get the RC as high as 80% even in the absence of any RSOI in the chiral QD. For the finite RSOI, the gate-voltage induces an effective RSOI in the system since it acts as an electric field [80,81]. With the increase in the gate voltage, the induced RSOI through the external field becomes more effective compared to the RSOI in the ungated junctions. With the increasing Rashba phase, the RC gradually decreases for all finite gate voltages. Keeping in mind the inevitable presence of RSOI in such a QD-based junction, it is possible to achieve RC $\sim 70\%$ by tuning V_g for an optimum strength of ϕ_{RS} in our proposed QD-based JD, which is the highest RC of a JD reported so far for the nontransparent junction to the best of our knowledge. Also, by tuning the gate voltage from positive to negative values, or vice versa, we can determine the direction of the preferential current flow in our JD as shown in Fig. 7. We find, at a particular RSOI, $\mathcal{R}(eV_g) \simeq -\mathcal{R}(-eV_g)$, i.e., the RC is almost symmetric with respect to the zero gate voltage at any RSOI.

IV. SUMMARY AND CONCLUSION

To summarize, we have studied the JDE in a single energy level chiral QD-based junction. To calculate the Josephson current, we have employed the Keldysh nonequilibrium Green's function technique. We have found that the critical current in our JJ increases with the increase in RSOI strength. We show the JDE in our chiral QD-based JJ in the presence of RSOI and a magnetic field. Note that in our RSOI coupled QD junction, the simultaneous presence of the chirality and the magnetic field is not mandatory to achieve JDE, but they can enhance the rectification. In the presence of RSOI, the magnitude of the RC gets amplified, and most importantly, it results in a sign-changing behavior of the RC. Finally, we have shown that by tuning the QD energy level via an external gate potential, it is possible to get a giant JDE with $\mathcal{R} \sim 70\%$ at an optimal strength of RSOI in the presence of magnetic field.

From the experimental point of view, an estimation of the induced current is in order. Using the Biot-Savart law, the induced magnetic field is found to be $B' = \frac{\mu_0 I}{2r}$, where r is the radius of the single turn of a current-carrying helix. This induced magnetic field is proportional to the current following $B' = \lambda I$. Hence, comparing both relations, we obtain $\lambda = \frac{\mu_0}{2r}$. Considering the radius $r = 1$ nm, the induced field will be of the order of 10^{-3} Oe for a current $I = 0.5$ nA. However, in our work, the RSOI plays the main role for inducing the larger diode effect. The RSOI changes as per the material property. In the widely used materials for QDs like GaAs or InAs, the RSOI strength is found to be very small, $\sim 0.04 \times 10^{-11}$ eVm and 0.28×10^{-11} eVm, respectively [80,82–84], whereas in InSb, RSOI is relatively higher, $\sim 1.16 \times 10^{-11}$ eVm [85]. Therefore, for the semiconductor QD with low RSOI strength, the gate voltage could be tuned easily to achieve a very high RC, as mentioned above. Our present results support three major experimental works on the SDE of recent times: (i) reconfirming Refs. [2,3], the breaking of IS through Rashba materials can induce the JDE; (ii) by tuning the gate voltage

[64], the RC of the JD can be increased by a large amount; and (iii) even in the absence of an external magnetic field it is possible to have a weak Josephson diode effect [8,27,30]. All these newly verified results are now explored in our QD junction.

Finally, we emphasize that including RSOI in modern quantum systems can be supremely effective in studying more efficient JDE. Our RSOI coupled QD junction explains the JDE theoretically, in a more general way, with a highly efficient possibility of experimental fabrication since RSOI is unavoidable in such low-dimensional junctions [86]. The tunability of the external magnetic field, the superconducting phase difference, gate voltage, RSOI, and applications to a wide range of quantum materials and correlated systems, like spin qubits, spin-transistors, single electron transistors, topological materials, Dirac semimetals, superconductors, and many more [51], make our proposed QD-based JDs highly efficient for switching devices.

ACKNOWLEDGMENTS

APPENDIX A: CALCULATIONS OF KELDYSH GREEN'S FUNCTION AND THE TRANSPORT MATRIX

In this Appendix, we summarize some major steps of the calculation of the Keldysh Green's function and the transport matrix.

The self-energy included in the Dyson equation of motion for the Keldysh retarded Green's function is expressed in the basis $\{\epsilon_\uparrow, -\epsilon_\uparrow, \epsilon_\downarrow, -\epsilon_\downarrow\}$ as [44]

$$\Sigma^{\mathrm{r}} = \begin{pmatrix} 0 & t_{\mathrm{LR}} & V_{\mathrm{L}} \\ t_{\mathrm{LR}}^* & 0 & V_{\mathrm{R}} \\ V_{\mathrm{L}}^* & V_{\mathrm{R}}^* & 0 \end{pmatrix}, \tag{A1}$$

where

$$t_{\mathrm{LR}} = \begin{pmatrix} t_{\epsilon\uparrow,\epsilon\uparrow} & 0 & 0 & 0 \\ 0 & t_{-\epsilon\uparrow,-\epsilon\uparrow} & 0 & 0 \\ 0 & 0 & t_{\epsilon\downarrow,\epsilon\downarrow} & 0 \\ 0 & 0 & 0 & t_{-\epsilon\downarrow,-\epsilon\downarrow} \end{pmatrix}, \tag{A2}$$

$$V_{\mathrm{L}} = \begin{pmatrix} v_{\mathrm{L}}e^{i\frac{\Phi_{\mathrm{L}}}{2}} & 0 & 0 & 0 \\ 0 & -v_{\mathrm{L}}e^{-i\frac{\Phi_{\mathrm{L}}}{2}} & 0 & 0 \\ 0 & 0 & v_{\mathrm{L}}e^{i\frac{\Phi_{\mathrm{L}}}{2}} & 0 \\ 0 & 0 & 0 & -v_{\mathrm{L}}e^{-i\frac{\Phi_{\mathrm{L}}}{2}} \end{pmatrix}, \tag{A3}$$

and

$$V_{\mathrm{R}} = \begin{pmatrix} v_{\mathrm{R}}e^{i(\frac{\Phi_{\mathrm{R}}}{2}-\phi_{\mathrm{RS}})} & 0 & 0 & 0 \\ 0 & -v_{\mathrm{R}}e^{-i(\frac{\Phi_{\mathrm{R}}}{2}+\phi_{\mathrm{RS}})} & 0 & 0 \\ 0 & 0 & v_{\mathrm{R}}e^{i(\frac{\Phi_{\mathrm{R}}}{2}+\phi_{\mathrm{RS}})} & 0 \\ 0 & 0 & 0 & -v_{\mathrm{R}}e^{-i(\frac{\Phi_{\mathrm{R}}}{2}-\phi_{\mathrm{RS}})} \end{pmatrix}. \tag{A4}$$

Here, $t_{\mathrm{L(R)}}$ is the tunneling matrix and $V_{\mathrm{L(R)}}$ represents the coupling between the left (right) superconductor and the QD. The Keldysh retarded Green's function can be expressed in a block form like

$$g^{\mathrm{r}} = \begin{pmatrix} g_{\mathrm{LL}}^{\mathrm{r}} & 0 & 0 \\ 0 & g_{\mathrm{RR}}^{\mathrm{r}} & 0 \\ 0 & 0 & g_{\mathrm{dd}}^{\mathrm{r}} \end{pmatrix}, \tag{A5}$$

where

$$g_{\alpha\alpha}^{\mathrm{r}} = \begin{pmatrix} g_{\alpha\alpha,\epsilon\uparrow,\epsilon\uparrow}^{\mathrm{r}} & g_{\alpha\alpha,\epsilon\uparrow,-\epsilon\uparrow}^{\mathrm{r}} & 0 & 0 \\ g_{\alpha\alpha,-\epsilon\uparrow,\epsilon\uparrow}^{\mathrm{r}} & g_{\alpha\alpha,-\epsilon\uparrow,-\epsilon\uparrow}^{\mathrm{r}} & 0 & 0 \\ 0 & 0 & g_{\alpha\alpha,\epsilon\downarrow,\epsilon\downarrow}^{\mathrm{r}} & g_{\alpha\alpha,\epsilon\downarrow,-\epsilon\downarrow}^{\mathrm{r}} \\ 0 & 0 & g_{\alpha\alpha,-\epsilon\downarrow,\epsilon\downarrow}^{\mathrm{r}} & g_{\alpha\alpha,-\epsilon\downarrow,-\epsilon\downarrow}^{\mathrm{r}} \end{pmatrix} \tag{A6}$$

with $\alpha \in \mathrm{L/R}$. The retarded Green's function for each individual lead is expressed as $g_{\alpha\alpha,\epsilon\sigma,\epsilon\sigma}^{\mathrm{r}} = -i\pi\rho\rho_\alpha$ and $g_{\alpha\alpha,\pm\epsilon\sigma,\mp\epsilon\sigma}^{\mathrm{r}} = -i\pi\rho\rho_\alpha\sigma\Delta_0/(\epsilon + i\eta^+)$. Here, the density of states of the QD is taken as $\rho = 1$, and the density of states of the leads is given by

$$\rho_\alpha = \begin{cases} \dfrac{|\epsilon|}{\sqrt{\epsilon^2 - \Delta_0^2}}, & |\epsilon| > \Delta_0, \\[2ex] \dfrac{-i\epsilon}{\sqrt{\Delta_0^2 - \epsilon^2}}, & |\epsilon| < \Delta_0. \end{cases} \tag{A7}$$

The Green's function of the uncoupled QD is calculated as

$$
g_{dd}^r = \begin{pmatrix} \frac{1}{\epsilon+i\eta^+ - H_{QD,\uparrow\uparrow}} & 0 & 0 & 0 \\ 0 & \frac{1}{-\epsilon+i\eta^+ - H_{QD,\uparrow\uparrow}} & 0 & 0 \\ 0 & 0 & \frac{1}{\epsilon+i\eta^+ - H_{QD,\downarrow\downarrow}} & 0 \\ 0 & 0 & 0 & \frac{1}{-\epsilon+i\eta^+ - H_{QD\downarrow\downarrow}} \end{pmatrix}. \tag{A8}
$$

Using the Keldysh retarded Green's function g^r of the uncoupled system and the individual coupling matrices (V_L, V_R, t_{LR}), the self-energy of the system Σ^r is calculated using Dyson's equation of motion. Further, the Keldysh lesser Green's function $G^<$ is computed numerically using the fluctuation-dissipation theorem following $G^<(\epsilon) = -f(\epsilon)(G^r - G^a)$, where $G^a = [G^r]^\dagger$. Finally, we calculate the Josephson current self-consistently using the matrix components of the Green's function.

APPENDIX B: EFFECT OF ASYMMETRIC LEADS

In this Appendix, we study the effect of asymmetric superconducting leads on the current profiles.

To impose the asymmetry between the two leads in our JJ, we consider $\Delta_L = 1$ and $\Delta_R = 0.6$ and plot the current in terms of the phase difference in Fig. 8. We observe that the positive and negative critical currents are different from each other. Comparing with Fig. 3, it is clearly visible that for the asymmetric leads, the nonreciprocity in the Josephson current increases. Also, the negative current is now higher than the positive current, unlike the situation for the symmetric leads. We have also checked (not shown to avoid an increasing number of figures) that the corresponding RC of our diode also increases when the leads are asymmetric compared to that for the symmetric case.

APPENDIX C: DERIVATION OF CURRENT EXPRESSION

In this Appendix, we present an analytical expression for the Josephson current in the presence of RSOI. From Eq. (11) we find that the effect of Rashba interaction is included in the tunneling Hamiltonian. Therefore, using this effective Hamiltonian, we calculate an approximate analytical expression for the Josephson current in our model.

The current can be defined in terms of the free energy F of the system as [15,55]

$$
I = \frac{2e}{\hbar} \frac{\partial F}{\partial \Phi}, \tag{C1}
$$

where e is the electronic charge, and it is set as $e = 1$. It can also expressed in terms of the partition function Z as

$$
I = \frac{2e}{\hbar} \frac{\partial(-T \ln Z)}{\partial \Phi}. \tag{C2}
$$

Now explicitly writing the partition function of the junction, we derive the current as

$$
\begin{aligned}
I &= -\frac{2e}{\hbar} \frac{1}{\beta} \frac{\partial(\ln \text{Tr}[\exp^{-\beta\tilde{H}}])}{\partial \Phi} \\
&\simeq v_L \exp^{-i\frac{\phi_{RS}}{2}} \sin\left(\frac{\Phi + \phi_{RS}}{2}\right) \\
&\quad + v_L \exp^{i\frac{\phi_{RS}}{2}} \sin\left(\frac{\Phi - \phi_{RS}}{2}\right). \tag{C3}
\end{aligned}
$$

Collecting the real part of the above expression, we obtain the approximate relation for the CPR mentioned in the main text.

APPENDIX D: RECTIFICATION IN THE ABSENCE OF CHIRALITY

In our QD-based JJ, we consider the presence of RSOI, which eventually breaks the IS. The QD is modeled to have chirality, which also breaks the symmetry. To obtain the JDE, the chirality is not any necessary condition when RSOI is present. For confirmation, we present the behavior of RC as a function of Rashba phase in the absence of λ for different magnetic fields in Fig. 9. The qualitative nature of the RC with the variation of RSOI is quite similar to that in the presence of

FIG. 8. Josephson current I in units of $e\Delta_0$ as a function of the phase difference for the asymmetric JJ.
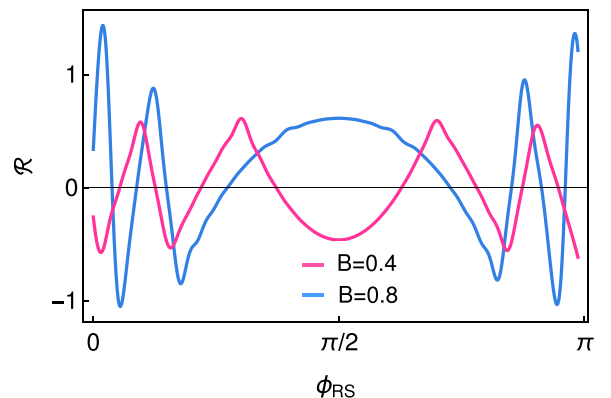
FIG. 9. RC ($\mathcal{R}\%$) vs Rashba phase in the absence of chirality.

chirality. Comparing with Fig. 5, we find that the magnitude of RC is higher in the presence of the chirality. However, the sign changing phenomenon is more prominent in the absence of the chirality. The sign of RC changes from positive to negative or vice versa with the change in Rashba phase. Thus, the sign and magnitude of the RC in our JD is sensitive to the chirality.

APPENDIX E: EFFECT OF DIRECT COUPLING

A direct coupling between the leads helps to tackle the effect of the RSOI analytically. In experimental fabrication, the coupling between the leads could be changed by forming the junction potential. Therefore, it is a controllable parameter in practice [74,83]. In the main text, we discuss all results for a particular value of the direct coupling strength. Now, we show its impact on the RC of our JD in Fig. 10. We find that the RC is oscillatory with respect to t_{LR} at a constant RSOI in the presence of the finite magnetic field. The direct coupling essentially plays the role of an extra channel in the QD junction.
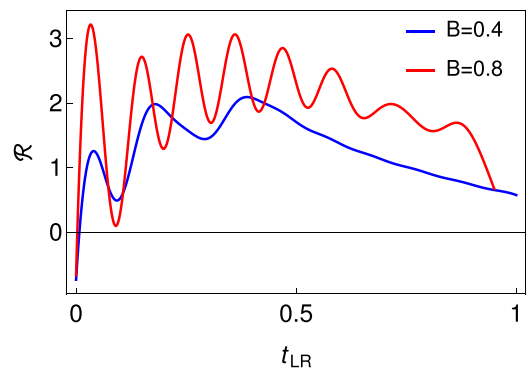
FIG. 10. RC ($\mathcal{R}\%$) vs hopping integral t_{LR} for $\phi_{RS} = \pi/4$.

Tuning the strength effectively leads to controlling the extra channel, which further modifies the tunneling phenomena and results in the oscillations. The oscillations increase with the increase in the magnetic field.

[1] F. Braun, Ueber die stromleitung durch schwefelmetalle, Ann. Phys. **229**, 556 (1875).

[2] F. Ando, Y. Miyasaka, T. Li, J. Ishizuka, T. Arakawa, Y. Shiota, T. Moriyama, Y. Yanase, and T. Ono, Observation of superconducting diode effect, Nature (London) **584**, 373 (2020).

[3] C. Baumgartner, L. Fuchs, A. Costa, S. Reinhardt, S. Gronin, G. C. Gardner, T. Lindemann, M. J. Manfra, P. E. Faria Junior, D. Kochan, J. Fabian, N. Paradiso, and C. Strunk, Supercurrent rectification and magnetochiral effects in symmetric Josephson junctions, Nat. Nanotechnol. **17**, 39 (2022).

[4] N. Murakami, S. Nagaosa and C. Zhang, Dissipationless quantum spin current at room temperature, Science **301**, 1348 (2003).

[5] K. Misaki and N. Nagaosa, Theory of the nonreciprocal Josephson effect, Phys. Rev. B **103**, 245302 (2021).

[6] Y. Zhang, Y. Gu, P. Li, J. Hu, and K. Jiang, General theory of Josephson diodes, Phys. Rev. X **12**, 041013 (2022).

[7] E. Strambini, M. Spies, N. Ligato, S. Ilić, M. Rouco, C. González-Orellana, M. Ilyn, C. Rogero, F. Bergeret, J. Moodera *et al.*, Superconducting spintronic tunnel diode, Nat. Commun. **13**, 2431 (2022).

[8] J.-X. Lin, P. Siriviboon, H. D. Scammell, S. Liu, D. Rhodes, K. Watanabe, T. Taniguchi, J. Hone, M. S. Scheurer, and J. I. A. Li, Zero-field superconducting diode effect in small-twist-angle trilayer graphene, Nat. Phys. **18**, 1221 (2022).

[9] H. Narita, J. Ishizuka, R. Kawarazaki, D. Kan, Y. Shiota, T. Moriyama, Y. Shimakawa, A. V. Ognev, A. S. Samardak, Y. Yanase *et al.*, Field-free superconducting diode effect in noncentrosymmetric superconductor/ferromagnet multilayers, Nat. Nanotechnol. **17**, 823 (2022).

[10] A. Daido, Y. Ikeda, and Y. Yanase, Intrinsic superconducting diode effect, Phys. Rev. Lett. **128**, 037001 (2022).

[11] T. de Picoli, Z. Blood, Y. Lyanda-Geller, and J. I. Väyrynen, Superconducting diode effect in quasi-one-dimensional systems, Phys. Rev. B **107**, 224518 (2023).

[12] J.-X. Hu, Z.-T. Sun, Y.-M. Xie, and K. T. Law, Josephson diode effect induced by valley polarization in twisted bilayer graphene, Phys. Rev. Lett. **130**, 266003 (2023).

[13] R. S. Souto, M. Leijnse, and C. Schrade, Josephson diode effect in supercurrent interferometers, Phys. Rev. Lett. **129**, 267702 (2022).

[14] Y.-J. Wei, H.-L. Liu, J. Wang, and J.-F. Liu, Supercurrent rectification effect in graphene-based Josephson junctions, Phys. Rev. B **106**, 165419 (2022).

[15] M. Davydova, S. Prembabu, and L. Fu, Universal Josephson diode effect, Sci. Adv. **8**, eabo0309 (2022).

[16] B. Zinkl, K. Hamamoto, and M. Sigrist, Symmetry conditions for the superconducting diode effect in chiral superconductors, Phys. Rev. Res. **4**, 033167 (2022).

[17] Y. V. Fominov and D. S. Mikhailov, Asymmetric higher-harmonic squid as a Josephson diode, Phys. Rev. B **106**, 134514 (2022).

[18] B. Lu, S. Ikegaya, P. Burset, Y. Tanaka, and N. Nagaosa, Tunable Josephson diode effect on the surface of topological insulators, Phys. Rev. Lett. **131**, 096001 (2023).

[19] S. Banerjee and M. S. Scheurer, Enhanced superconducting diode effect due to coexisting phases, Phys. Rev. Lett. **132**, 046003 (2024).

[20] A. Zazunov, R. Egger, T. Jonckheere, and T. Martin, Anomalous Josephson current through a spin-orbit coupled quantum dot, Phys. Rev. Lett. **103**, 147004 (2009).

[21] P. Chatterjee and P. Dutta, Quasiparticles-mediated thermal diode effect in Weyl Josephson junctions, arXiv:2312.05008.

[22] Q. Cheng and Q.-F. Sun, Josephson diode based on conventional superconductors and a chiral quantum dot, Phys. Rev. B **107**, 184511 (2023).

[23] G. L. J. A. Rikken, J. Fölling, and P. Wyder, Electrical magnetochiral anisotropy, Phys. Rev. Lett. **87**, 236602 (2001).

[24] N. N. Tokura and N. Nagaosa, Nonreciprocal responses from non-centrosymmetric quantum materials, Nat. Commun. **9**, 3740 (2018).

[25] B. Pal, A. Chakraborty, P. K. Sivakumar, M. Davydova, A. K. Gopi, A. K. Pandeya, J. A. Krieger, Y. Zhang, M. Date, S. Ju, N. Yuan, N. B. M. Schröter, L. Fu, and S. S. P. Parkin, Josephson diode effect from cooper pair momentum in a topological semimetal, Nat. Phys. **18**, 1228 (2022).

[26] N. F. Yuan and L. Fu, Supercurrent diode effect and finite-momentum superconductors, Proc. Natl. Acad. Sci. USA **119**, e2119548119 (2022).

[27] H. D. Scammell, J. I. A. Li, and M. S. Scheurer, Theory of zero-field superconducting diode effect in twisted trilayer graphene, 2D Mater. **9**, 025027 (2022).

[28] J. J. He, Y. Tanaka, and N. Nagaosa, A phenomenological theory of superconductor diodes, New J. Phys. **24**, 053014 (2022).

[29] L. Bauriedl, C. Bäuml, L. Fuchs, C. Baumgartner, N. Paulik, J. M. Bauer, K.-Q. Lin, J. M. Lupton, T. Taniguchi, K. Watanabe, C. Strunk, and N. Paradiso, Supercurrent diode effect and magnetochiral anisotropy in few-layer NbSe$_2$, Nat. Commun. **13**, 4266 (2022).

[30] H. Wu, Y. Wang, Y. Xu, P. K. Sivakumar, C. Pasco, U. Filippozzi, S. S. P. Parkin, Y.-J. Zeng, T. McQueen, and M. N. Ali, The field-free Josephson diode in a van der Waals heterostructure, Nature (London) **604**, 653 (2022).

[31] H. F. Legg, D. Loss, and J. Klinovaja, Superconducting diode effect due to magnetochiral anisotropy in topological insulators and Rashba nanowires, Phys. Rev. B **106**, 104501 (2022).

[32] K. Chen, B. Karki, and P. Hosur, Intrinsic superconducting diode effects in tilted Weyl and Dirac semimetals, Phys. Rev. B **109**, 064511 (2024).

[33] A. Costa, J. Fabian, and D. Kochan, Microscopic study of the Josephson supercurrent diode effect in Josephson junctions based on two-dimensional electron gas, Phys. Rev. B **108**, 054522 (2023).

[34] M. Trahms, L. Melischek, J. F. Steiner, B. Mahendru, I. Tamir, N. Bogdanoff, O. Peters, G. Reecht, C. B. Winkelmann, F. von Oppen, and K. J. Franke, Diode effect in Josephson junctions with a single magnetic atom, Nature (London) **615**, 628 (2023).

[35] J. J. He, Y. Tanaka, and N. Nagaosa, The supercurrent diode effect and nonreciprocal paraconductivity due to the chiral structure of nanotubes, Nat. Commun. **14**, 3330 (2023).

[36] B. Turini, S. Salimian, M. Carrega, A. Iorio, E. Strambini, F. Giazotto, V. Zannier, L. Sorba, and S. Heun, Josephson diode effect in high-mobility InSb nanoflags, Nano Lett. **22**, 8502 (2022).

[37] T. Liu, M. Smith, A. V. Andreev, and B. Z. Spivak, Giant nonreciprocity of current-voltage characteristics of noncentrosymmetric superconductor–normal metal–superconductor junctions, Phys. Rev. B **109**, L020501 (2024).

[38] A. Soori, Josephson diode effect in junctions of superconductors with band asymmetric metals, arXiv:2312.14084.

[39] J. Cayao, N. Nagaosa, and Y. Tanaka, Enhancing the Josephson diode effect with Majorana bound states, Phys. Rev. B **109**, L081405 (2024).

[40] Z. Liu, L. Huang, and J. Wang, Josephson diode effect in topological superconductor, arXiv:2311.09009.

[41] Y.-F. Sun, Y. Mao, and Q.-F. Sun, Design of Josephson diode based on magnetic impurity, Phys. Rev. B **108**, 214519 (2023).

[42] C. Ortega-Taberner, A.-P. Jauho, and J. Paaske, Anomalous Josephson current through a driven double quantum dot, Phys. Rev. B **107**, 115165 (2023).

[43] Q. F. Sun, J. Wang, and T. H. Lin, Control of the supercurrent in a mesoscopic four-terminal Josephson junction, Phys. Rev. B **62**, 648 (2000).

[44] Q. F. Sun, J. Wang, and H. Guo, Quantum transport theory for nanostructures with Rashba spin-orbital interaction, Phys. Rev. B **71**, 165310 (2005).

[45] L. Dell'Anna, A. Zazunov, R. Egger, and T. Martin, Josephson current through a quantum dot with spin-orbit coupling, Phys. Rev. B **75**, 085305 (2007).

[46] H.-Z. Tang, Y.-T. Zhang, and J.-J. Liu, Josephson current through a quantum dot coupled to a Majorana zero mode, J. Phys.: Condens. Matter **28**, 175301 (2016).

[47] A. Soori, DC Josephson effect in superconductor-quantum dot-superconductor junctions, arXiv:1905.01925.

[48] D. Loss and D. P. DiVincenzo, Quantum computation with quantum dots, Phys. Rev. A **57**, 120 (1998).

[49] G.-J. Qiao, Z.-L. Zhang, S.-W. Li, and C. P. Sun, Controlling superconducting transistor by coherent light, arXiv:2305.04442.

[50] S. Lee, Y. Lee, E. B. Song, and T. Hiramoto, Observation of single electron transport via multiple quantum states of a silicon quantum dot at room temperature, Nano Lett. **14**, 71 (2014).

[51] A. Hirohata, K. Yamada, Y. Nakatani, I.-L. Prejbeanu, B. Diény, P. Pirro, and B. Hillebrands, Review on spintronics: Principles and device applications, J. Magn. Magn. Mater. **509**, 166711 (2020).

[52] H. Linke, Quantum dots - seeds of nanoscience, R. Swed. Acad. Sci. (2023).

[53] A. Y. Bychkov and E. I. Rashba, Properties of a 2D electron gas with lifted spectral degeneracy, JETP Lett. **39**, 66 (1984).

[54] T. Yokoyama, M. Eto, and Y. V. Nazarov, Anomalous Josephson effect induced by spin-orbit interaction and Zeeman effect in semiconductor nanowires, Phys. Rev. B **89**, 195407 (2014).

[55] A. Rasmussen, J. Danon, H. Suominen, F. Nichele, M. Kjaergaard, and K. Flensberg, Effects of spin-orbit coupling and spatial symmetries on the Josephson current in SNS junctions, Phys. Rev. B **93**, 155406 (2016).

[56] S. LaShell, B. A. McDougall, and E. Jensen, Spin splitting of an AU(111) surface state band observed with angle resolved photoelectron spectroscopy, Phys. Rev. Lett. **77**, 3419 (1996).

[57] K. Ishizaka, S. Bahramy, M. H. Murakawa, M. Sakano, T. Shimojima, T. Sonobe, K. Koizumi, S. Shin, H. Miyahara, A. Kimura, K. Miyamoto, H. Okuda, H. Namatame, M. Taniguchi, R. Arita, N. Nagaosa, K. Kobayashi, Y. Murakami, R. Kumai, Y. Kaneko *et al.*, Giant Rashba-type spin splitting in bulk BiTeI, Nat. Mater. **10**, 521 (2011).

[58] J. Nitta, T. Akazaki, H. Takayanagi, and T. Enoki, Gate control of spin-orbit interaction in an inverted In$_{0.53}$Ga$_{0.47}$As/In$_{0.52}$Al$_{0.48}$As heterostructure, Phys. Rev. Lett. **78**, 1335 (1997).

[59] M. Ben Shalom, M. Sachs, D. Rakhmilevitch, A. Palevski, and Y. Dagan, Tuning spin-orbit coupling and superconductivity at the SrTiO$_3$/LaAlO$_3$ interface: A magnetotransport study, Phys. Rev. Lett. **104**, 126802 (2010).

[60] Y. Mao, Q. Yan, Y.-C. Zhuang, and Q.-F. Sun, Universal spin superconducting diode effect from spin-orbit coupling, arXiv:2306.09113.

[61] L. V. Keldysh, Diagram technique for nonequilibrium processes, JETP Lett. (USSR) **47**, 1515 (1964).

[62] G. D. Mahan, *Many Particle Physics*, 3rd ed. (Plenum, New York, 2000).

[63] J. A. van Dam, Y. V. Nazarov, E. P. A. M. Bakkers, S. De Franceschi, and L. P. Kouwenhoven, Supercurrent reversal in quantum dots, Nature (London) **442**, 667 (2006).

[64] M. Gupta, G. Graziano, M. Pendharkar, J. T. Dong, C. P. Dempsey, C. Palmstrøm, and V. S. Pribiag, Gate-tunable super-conducting diode effect in a three-terminal Josephson device, Nat. Commun. **14**, 3078 (2023).

[65] I. G. Zacharia, D. Goldhaber-Gordon, G. Granger, M. A. Kastner, Y. B. Khavin, H. Shtrikman, D. Mahalu, and U. Meirav, Temperature dependence of Fano line shapes in a weakly coupled single-electron transistor, Phys. Rev. B **64**, 155311 (2001).

[66] Z. Y. Zeng, F. Claro, and A. Pérez, Fano resonances and Aharonov-Bohm effects in transport through a square quantum dot molecule, Phys. Rev. B **65**, 085308 (2002).

[67] Z. Ma, Y. Zhu, X.-Q. Li, T. H. Lin, and Z.-B. Su, Photon-assisted Fano resonance and corresponding shot noise in a quantum dot, Phys. Rev. B **69**, 045302 (2004).

[68] K. Bhattacharyya, D. Debnath, and A. Chatterjee, Rashba effect on finite temperature magnetotransport in a dissipative quantum dot transistor with electronic and polaronic interactions, Sci. Rep. **13**, 5500 (2023).

[69] A.-P. Jauho, N. S. Wingreen, and Y. Meir, Time-dependent transport in interacting and noninteracting resonant-tunneling systems, Phys. Rev. B **50**, 5528 (1994).

[70] S. Datta, *Electronic Transport in Mesoscopic Systems* (Cambridge University Press, United Kingdom, 1997).

[71] R. Kubo, The fluctuation-dissipation theorem, Rep. Prog. Phys. **29**, 255 (1966).

[72] A. Kamenev, *Field Theory of Non-Equilibrium Systems* (Cambridge University Press, United Kingdom, 2011).

[73] N. Lotfizadeh, B. Pekerten, P. Yu, W. Strickland, A. Matos-Abiague, and J. Shabani, Superconducting diode effect sign change in epitaxial Al-InAs Josepshon junctions, Commun. Phys. **7**, 120 (2024).

[74] W. Mayer, M. C. Dartiailh, J. Yuan, K. S. Wickramasinghe, E. Rossi, and J. Shabani, Gate controlled anomalous phase shift in Al/InAs Josephson junctions, Nat. Commun. **11**, 212 (2020).

[75] A. Assouline, C. Feuillet-Palma, N. Bergeal, T. Zhang, A. Mottaghizadeh, A. Zimmers, E. Lhuillier, M. Eddrie, P.

Atkinson, M. Aprili *et al.*, Spin-orbit induced phase-shift in Bi$_2$Se$_3$ Josephson junctions, Nat. Commun. **10**, 126 (2019).

[76] A. Buzdin, Peculiar properties of the Josephson junction at the transition from 0 to π state, Phys. Rev. B **72**, 100501(R) (2005).

[77] A. Buzdin, Direct coupling between magnetism and superconducting current in the Josephson φ_0 junction, Phys. Rev. Lett. **101**, 107005 (2008).

[78] I. V. Krive, A. M. Kadigrobov, R. I. Shekhter, and M. Jonson, Influence of the Rashba effect on the Josephson current through a superconductor/Luttinger liquid/superconductor tunnel junction, Phys. Rev. B **71**, 214516 (2005).

[79] A. A. Reynoso, G. Usaj, C. A. Balseiro, D. Feinberg, and M. Avignon, Anomalous Josephson current in junctions with spin polarizing quantum point contacts, Phys. Rev. Lett. **101**, 107001 (2008).

[80] J. Hong, J. Lee, S. Joo, K. Rhie, B.-C. Lee, J. Lee, S.-Y. An, J. Kim, and K.-H. Shin, Control of the spin-orbit coupling by gate voltage in semiconductor fet structures, J. Korean Phys. Soc. **45**, 197 (2004).

[81] A. Iorio, M. Rocci, L. Bours, M. Carrega, V. Zannier, L. Sorba, S. Roddaro, F. Giazotto, and E. Strambini, Vectorial control of the spin–orbit interaction in suspended InAs nanowires, Nano Lett. **19**, 652 (2019).

[82] P. S. Eldridge, W. J. H. Leyland, P. G. Lagoudakis, O. Z. Karimov, M. Henini, D. Taylor, R. T. Phillips, and R. T. Harley, Temperature dependence of Rashba spin-orbit coupling in quantum wells, arXiv:0707.4493.

[83] J. B. Miller, D. M. Zumbühl, C. M. Marcus, Y. B. Lyanda-Geller, D. Goldhaber-Gordon, K. Campman, and A. C. Gossard, Gate-controlled spin-orbit quantum interference effects in lateral transport, Phys. Rev. Lett. **90**, 076807 (2003).

[84] G. L. Chen, J. Han, T. T. Huang, S. Datta, and D. B. Janes, Observation of the interfacial-field-induced weak antilocalization in InAs quantum structures, Phys. Rev. B **47**, 4084 (1993).

[85] S. K. Greene, J. Singleton, P. Sobkowicz, T. D. Golding, M. Pepper, J. A. A. J. Perenboom, and J. Dinan, Subband occupancies and zero-field spin splitting in InSb-CdTe heterojunctions: Magnetotransport experiments and self-consistent calculations, Semicond. Sci. Technol. **7**, 1377 (1992).

[86] A. Manchon, H. C. Koo, J. Nitta, S. M. Frolov, and R. A. Duine, New perspectives for Rashba spin–orbit coupling, Nat. Mater. **14**, 871 (2015).